Overexpression of Fibroblast Growth Factor-10 during Both Inflammatory and Fibrotic Phases Attenuates Bleomycin-induced Pulmonary Fibrosis in Mice

Varsha V. Gupte[1]*, Suresh K. Ramasamy[1]*, Raghava Reddy[1], Jooeun Lee[1], Paul H. Weinreb[2], Shelia M. Violette[3], Andreas Guenther[4], David Warburton[1], Barbara Driscoll[1], Parviz Minoo[5], and Saverio Bellusci[1]

[1]Developmental Biology Program, Division of Surgery, Saban Research Institute of Children's Hospital Los Angeles, University of Southern California Keck School of Medicine, Los Angeles, California; [2]Biogen Idec, Inc., and [3]Stromedix, Inc., Cambridge, Massachusetts; [4]University of Giessen Lung Center, Department of Internal Medicine II, University of Giessen, Giessen, Germany; and [5]Department of Pediatrics, Women's and Children's Hospital, University of Southern California Keck School of Medicine, Los Angeles, California

***Rationale*: Fibroblast growth factor-10 (FGF10) controls survival, proliferation, and differentiation of distal-alveolar epithelial progenitor cells during lung development.**

***Objectives*: To test for the protective and regenerative effect of *Fgf10* overexpression in a bleomycin-induced mouse model of pulmonary inflammation and fibrosis.**

***Methods*: In *SP-C-rtTA*; *tet(O)Fgf10* double-transgenic mice, lung fibrosis was induced in 2-month-old transgenic mice by subcutaneous delivery of bleomycin (BLM), using an osmotic minipump for 1 week. Exogenous *Fgf10* expression in the alveolar epithelium was induced for 7 days with doxycycline during the first, second, and third weeks after bleomycin pump implantation, and lungs were examined at 28 days.**

***Measurements and Main Results*: *Fgf10* overexpression during Week 1 (inflammatory phase) resulted in increased survival and attenuated lung fibrosis score and collagen deposition. In these *Fgf10*-overexpressing mice, an increase in regulatory T cells and a reduction in both transforming growth factor-β_1 and matrix metalloproteinase-2 activity were observed in bronchoalveolar lavage fluids whereas the number of surfactant protein C (SP-C)–positive, alveolar epithelial type II cells (AEC2) was markedly elevated. Analysis of SP-C and TUNEL (terminal deoxynucleotidyltransferase dUTP nick end labeling) double-positive cells and isolation of AEC2 from lungs overexpressing *Fgf10* demonstrated increased AEC2 survival. Expression of *Fgf10* during Weeks 2 and 3 (fibrotic phase) showed significant attenuation of the lung fibrosis score and collagen deposition.**

***Conclusions*: In the bleomycin model of lung inflammation and fibrosis, *Fgf10* overexpression during both the inflammatory and fibrotic phases results in a greatly reduced extent of lung fibrosis, suggesting that FGF10 may be useful as a novel approach to the treatment of pulmonary fibrosis.**

Keywords: bleomycin; fibrosis; *Fgf10*; transforming growth factor-β_1; alveolar epithelial progenitors

AT A GLANCE COMMENTARY

Scientific Knowledge on the Subject

Fibroblast growth factor-10 (FGF10) plays a crucial role in lung development. It is also up-regulated during hyperoxia–induced injury in adult mice. Whether FGF10 has a role in repair in lung fibrosis has not been studied.

What This Study Adds to the Field

This study shows that in the bleomycin model of lung inflammation and fibrosis, *Fgf10* overexpression during both the inflammatory and fibrotic phases results in a greatly reduced extent of lung fibrosis, suggesting that FGF10 may be useful as a novel approach to the treatment of pulmonary fibrosis.

Idiopathic pulmonary fibrosis, or IPF, is a devastating disease for which no cure exists at the moment. On average, patients with IPF survive 2 to 4 years after diagnosis (1) and this is partly explained by our limited understanding of the pathomechanism of this disease and the lack of effective treatment. Because of the visible signs of inflammation (lymphoplasmacellular infiltration of septae, neutrophilic alveolitis, and slightly enlarged lymph nodes) in IPF lungs, steroids and immunosuppressants have been extensively used in the past—however, with limited success (2). Chronic injury and apoptosis of alveolar type II cells (AEC2) have been suggested to underlie the evolution and progression of the disease (3), ultimately resulting in fibroblast proliferation, increased matrix (collagen) deposition, and loss of regular alveolar structure (4).

A strategy to attenuate or reverse the manifestations of IPF would involve maintenance of epithelial integrity during injury, particularly protection of alveolar progenitor cells, regeneration of AEC2, restoration of the damaged extracellular matrix, and clearance of alveolar fluid. Interestingly, secreted products of AEC2 such as prostaglandin E_2 are known to inhibit fibroblast proliferation and collagen synthesis (5). Intratracheal administration of isolated AEC2 during the fibrotic phase has been shown to significantly attenuate bleomycin-induced lung fibrosis (6), demonstrating that targeting the epithelium will likely be an important key for novel approaches to the treatment of IPF.

We propose that one such approach could be fibroblast growth factor-10 (FGF10), which has been shown to control survival and proliferation of endogenous distal alveolar progenitor cells during lung development (7, 8). FGF10 binds predominantly to the receptor isoform FGFR2b, which has been reported to be critical for the alveolar repair process after hyperoxic injury *in vivo* (9). Interleukin-1β mediated up-regulation of the expression of FGF7, another member of the FGF family that also acts through FGFR2b, is decreased in human fibroblasts from IPF versus normal lung (10), suggesting that the abnormal epithelial

(*Received in original form November 28, 2008; accepted in final form June 3, 2009*)

* These authors have contributed equally to this work.

Supported by National Institutes of Health grants HL086322 and HL074832 (to S.B.) and HL060231 (to P.M.).

Correspondence and requests for reprints should be addressed to Saverio Bellusci, Ph.D., Saban Research Institute of Children's Hospital Los Angeles, Los Angeles, CA 90027. E-mail: sbellusci@chla.usc.edu; and to Parviz Minoo, Ph.D., Women's and Children's Hospital, Los Angeles, CA 90033. E-mail: minoo@usc.edu

This article has an online supplement, which is accessible from this issue's table of contents at www.atsjournals.org

Am J Respir Crit Care Med Vol 180. pp 424–436, 2009
Originally Published in Press as DOI: 10.1164/rccm.200811-1794OC on June 4, 2009
Internet address: www.atsjournals.org

repair observed in IPF may be partly explained by low levels of critical FGFR2b ligands further supporting IPF progression. In alveolar epithelial cells, FGF10 promotes differentiation, migration, and wound healing and prevents oxidant- and cyclic stretch–induced DNA damage (11–13).

In this study, we used mice engineered for the inducible expression of *Fgf10* in the alveolar epithelium to demonstrate the protective as well as regenerative effect of *Fgf10* overexpression in a bleomycin-induced lung inflammation and fibrosis model. Our results indicate that *Fgf10* overexpression during both the inflammatory and fibrotic phases leads to a clear attenuation of fibrosis. This attenuation is likely the consequence of increased resistance of AEC2 to injury by promoting their survival. In future, the use of FGF10 should therefore be evaluated as a potential approach to the treatment of IPF.

METHODS

See the online supplement for a detailed description of METHODS.

Bleomycin Treatment for the Induction of Fibrosis

The *SP-C-rtTA*; *tet(O)Fgf10* mice used in this study were obtained from J. Whitsett (Cincinnati Children's Hospital Medical Center, Cincinnati, OH) (14). All animal studies were performed according to the protocols and guidelines of the institutional animal care and use committee. Double-transgenic *rtTA*; *tet(O)Fgf10* mice that overexpress *Fgf10* under the control of the tetracycline reverse transcriptional activator (rtTA) expressed from the ubiquitous *Rosa26* promoter (15) were used for the isolation of AEC2. For bleomycin delivery, a micro-osmotic pump containing bleomycin sulfate was surgically inserted into the mid-back region of 8-week-old female *SP-C-rtTA*; *tet(O)Fgf10* mice.

Histological Analysis

Mouse lung sections were stained either with hematoxylin–eosin or, for collagen, by Masson's trichrome staining to determine the extent of fibrosis. Immunohistochemistry was also done with antibodies for surfactant protein (SP)-C and apoptosis studies (TUNEL, terminal deoxynucleotidyltransferase dUTP nick end labeling). $\alpha_v\beta_6$ Immunostaining was performed with a chimeric version of the anti-$\alpha_v\beta_6$ primary antibody, 6.2G2 (16).

Fibrosis Score and Collagen Quantification

Morphological changes in fibrotic lungs were quantified according to a numerical scale as described by Ashcroft and colleagues (17). Total soluble collagen was assessed by Sircol collagen assay kit (Biocolor Ltd, Carrickfergus, Ireland) according to the manufacturer's instructions.

Inflammatory Cell Counts, Transforming Growth Factor-β_1 Activity, and Flow Cytometry of Bronchoalveolar Lavage Fluid Samples

Bronchoalveolar lavage fluid (BALF) was collected as previously described to assess the total number of macrophages and transforming growth factor (TGF)-β_1 content at 3-, 7-, and 14-day time points. Seven days after pump implantation, BALF was collected from bleomycin-treated mice and the lavage cells were stained with antibodies for CD4–FITC, CD25–APC, and Foxp3–PE and the appropriate isotype controls (from Ebioscience, San Diego, CA). Flow cytometry was done and populations of $CD4^+CD25^+Foxp3^+$ cells were analyzed in individual BAL samples. T-regulatory (Treg) cell frequency is reported as a percentage of $CD4^+$ cells. For the assessment of TGF-β_1 bioactivity, murine lung epithelial (MLE12) cells stably transfected with the *plasminogen activator inhibitor* (*PAI-1*) promoter driving luciferase expression were used.

Real-time Polymerase Chain Reaction (PCR) and Reverse Transcriptase-PCR Analysis

cDNA (25 pg) was used for real-time polymerase chain reaction (PCR) analysis, using a FastStart TaqMan probe master kit (Roche, Indianapolis, IN), in Roche LightCycler 1.5. Primers and probes were designed with ProbeFinder version 2.20 (Roche). One microgram of cDNA and 10 pg of primers were used in reverse transcriptase-PCRs.

Western Blotting and Sodium Dodecyl Sulfate Polyacrylamide Gel Electrophoresis Zymography

Immunoblotting was done with lung homogenates and phospho-SMAD3 antibody (from Cell Signaling Technology, Danvers, MA) or with β-actin antibody (Cell Signaling Technology). Gelatin zymograms were run with BALF to measure MMP-2 activity.

Isolation of Alveolar Type II Cells

Murine AEC2 were isolated according to Lee and colleagues (18). AEC2 cultured for 40 hours in chamber slides were stained for cytokeratin, vimentin, and SP-C to detect cell type–specific protein expression.

Data Presentation and Statistical Analysis

Data are expressed as means ± SD unless otherwise stated. Statistical analyses were performed on the data through two-factor analysis of variance between more than two groups and with the Student *t* test for comparisons of two groups, using Excel (Microsoft, Redmond, WA). *P* values less than 0.05 were considered significant.

RESULTS

Fgf10-overexpressing Mice Exhibit Survival Advantage in Response to Bleomycin

Bleomycin (BLM) is a well-established agent for inducing pulmonary inflammation and fibrosis. We chose subcutaneous administration of bleomycin, using micro-osmotic pumps, for our experiments as this technique for a limited time period closely mimicks the progressive nature of fibrosis observed in human patients. In the C57BL/6 background 25 to 50% mortality has been reported in lung fibrosis induced with comparable BLM doses (19). *Fgf10* is overexpressed in *SP-C-rtTA*; *tet(O)Fgf10* mice by administering a doxycycline (DOX) diet. Our experimental scheme and the resulting four groups of mice are depicted in Figures 1A and 1B. Control mice were treated with saline (SAL). The time of implantation of micro-osmotic pumps in *SP-C-rtTA*; *tet(O)Fgf10* mice is designated as Day 0. The mice were killed 28 days after pump implantation.

Our results show that our double-transgenic system is not leaky, as exogenous *Fgf10* expression using previously reported primers (14) is observed only on DOX treatment (Figure 1C). Quantification of *Fgf10* expression by real-time PCR (Figure 1D) indicated an 11-fold increase in DOX^+ versus DOX^- animals. From Figure 1, it may be seen that all saline-treated as well as bleomycin-treated transgenic mice given doxycycline in the first week survived the 28-day observation period compared with 38% survival of BLM/DOX^- mice, in which FGF10 was not overexpressed. Mice in the BLM/DOX^- group started to die after the second week (Figure 1E) of pump implantation. Each bleomycin-treated group consisted of eight mice (n = 8) and saline-treated groups had four mice each (n = 4). Thus, *Fgf10* overexpression resulted in an increase in survival of BLM-treated mice.

Overexpression of *Fgf10* Results in Attenuation of Lung Fibrosis

Fgf10 overexpression during the inflammatory phase leads to a reduction in fibrotic scarring and collagen deposition in the lungs. Histological analysis of hematoxylin and eosin–stained sections of mouse lungs at the 28-day time point revealed no signs of alveolar remodeling or fibrosis in either of the saline groups (SAL/DOX^- and SAL/DOX^+) (Figures 2A and 2B). In contrast, there was a large amount of extracellular matrix

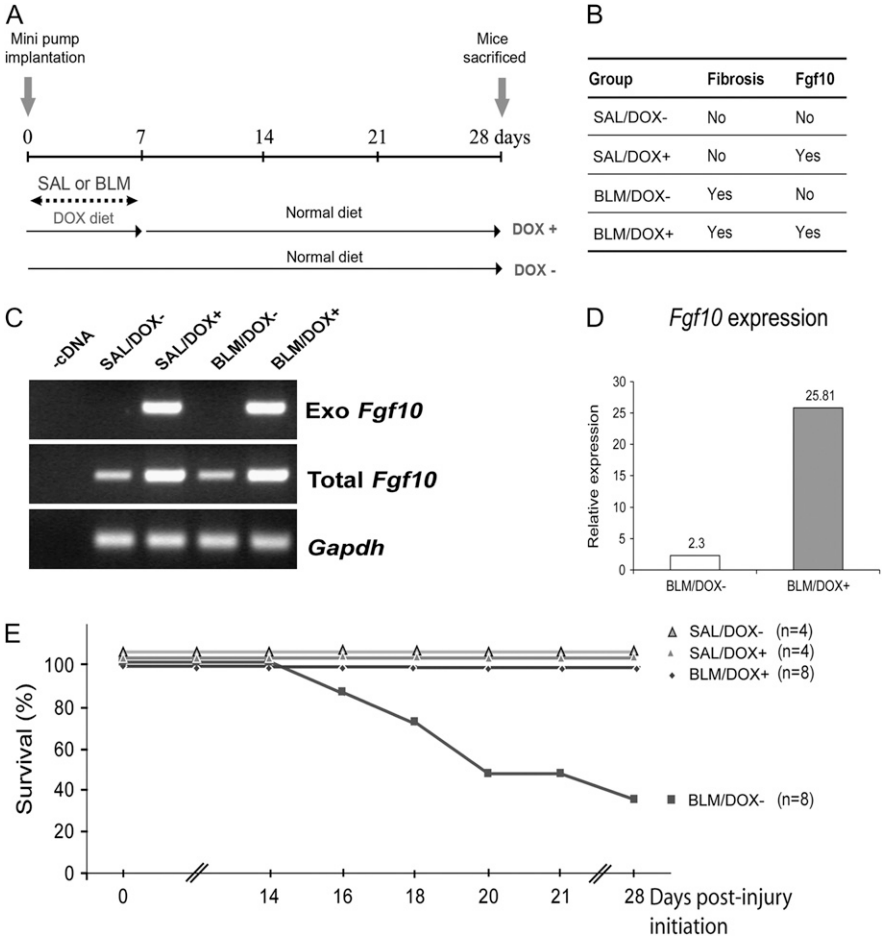

Group	Fibrosis	Fgf10
SAL/DOX-	No	No
SAL/DOX+	No	Yes
BLM/DOX-	Yes	No
BLM/DOX+	Yes	Yes

Figure 1. Experimental scheme and survival curve of bleomycin-administered *SP-C-rtTA*; *tet(O)Fgf10* mice. (*A*) Minipumps containing either bleomycin (BLM) or saline (SAL) were subcutaneously inserted into 2-month-old *SP-C-rtTA*; *tet(O)Fgf10* mice. *Fgf10* overexpression was triggered for a period of 7 days by feeding the mice a doxycycline diet (DOX$^+$). Control mice were fed a normal diet (DOX$^-$) throughout the experiment. For analysis, these mice were killed 28 days after implantation of the pumps (designated as Day 0). (*B*) The four groups of double-transgenic mice categorized on the basis of the type of treatment and diet they received (SAL or BLM). The BLM/DOX$^+$ group is the experimental group, in which fibrosis was induced and *Fgf10* was overexpressed. The other three groups are the controls. (*C*) Exogenous *Fgf10* expression in lungs on Day 7 is specifically detected in the presence of doxycycline by RT-PCR. (*D*) Quantification of total *Fgf10*, using real-time PCR, in BLM/DOX$^+$ versus BLM/DOX$^-$ lungs 7 days after pump implantation. (*E*) *Fgf10*-overexpressing mice (BLM/DOX$^+$; n = 8) show 100% survival after bleomycin treatment (0.1 mg/g mouse weight) compared with only about 38% survival among BLM-treated mice that do not overexpress *Fgf10* (BLM/DOX$^-$; n = 8). Mice in the saline-treated control groups (n = 4 each) showed 100% survival.

deposition and profound lymphoplasmacellular infiltration in lungs from the BLM/DOX$^-$ group (Figure 2C). Some scarring and inflammation were also observed in lungs from the BLM/DOX$^+$ group. However, this was restricted to the subpleural regions of the distal lung wherein marginal interstitial thickening and the presence of some fibrotic zones were observed in the lungs from the *Fgf10*-overexpressing (BLM/DOX$^+$) group (Figure 2D). These hematoxylin and eosin–stained sections were further analyzed for fibrosis scoring, using Ashcroft's method (17), to compare the extent of fibrosis in BLM-treated DOX$^+$ versus DOX$^-$ lungs. *Fgf10* overexpression led to a twofold reduction of Ashcroft's fibrosis score in response to BLM treatment (Figure 2E) ($P < 0.01$, n = 3).

Total collagen content in the lung can be used as a measure of the extent of fibrosis. Increased amounts of extracellular matrix deposition could also be observed in the sections stained for collagen with Masson's trichrome in the bleomycin control group (Figure 3C). The BLM/DOX$^-$ group exhibited a significant increase in total collagen over the BLM/DOX$^+$ group as quantified by the Sircol assay (Figure 3E) ($P < 0.01$, n = 3).

BLM-induced Early Inflammatory Response Is Affected by *Fgf10* Overexpression

Inflammation occurs after BLM injury and is thought to contribute to the fibrotic process (20). Two weeks after bleomycin administration, the inflammatory response has been reported to wane and collagen deposition can be detected (21). Thus there is an increase in the accumulation of collagen for 4–6 weeks, which thereafter declines. To analyze the inflammatory response over time, BALF was collected from mice at the 3- and 7-day time points. The total numbers of cells were counted and a differential cell count was also performed for four mice from each group. Our results indicated that the BLM/DOX$^-$ group as well as the BLM/DOX$^+$ group showed large amounts of inflammation and cell infiltration in BALF compared with the BALF of saline-treated control animals. No significant difference regarding total amount of cells as well as the percentage of macrophages, lymphocytes, and neutrophils was observed between the DOX$^+$ and DOX$^-$ bleomycin groups (Figure 4). We further explored potential changes in T-cell subpopulations. In particular, the subpopulation of CD4$^+$CD25$^+$Foxp3$^+$ Treg cells has been shown in previous studies to be essential for the control of immunological tolerance and prevention of autoimmunity (22). In humans, defective function of Treg cells in the BAL highly correlates with parameters of disease severity in patients with IPF, suggesting a role for Treg cells in the fibrotic process (23).

However, when BALF samples from bleomycin-treated mice after 7 days were analyzed for the percentage of Treg cells, a twofold increase was observed in the BLM/DOX$^+$ group as compared with the BLM/DOX$^-$ group (4.82 ± 0.99 vs. 2.45 ± 0.62%, respectively; n = 3, $P < 0.05$). Therefore, even though the primary analysis of the inflammatory cells did not reveal any significant difference between the BLM/DOX$^-$ and BLM/DOX$^+$ groups, an increased Treg cell subpopulation via a suppressed inflammatory response may contribute to the observed attenuation of lung fibrosis. How FGF10 is capable of triggering the increase in Treg cells will need to be explored in further studies.

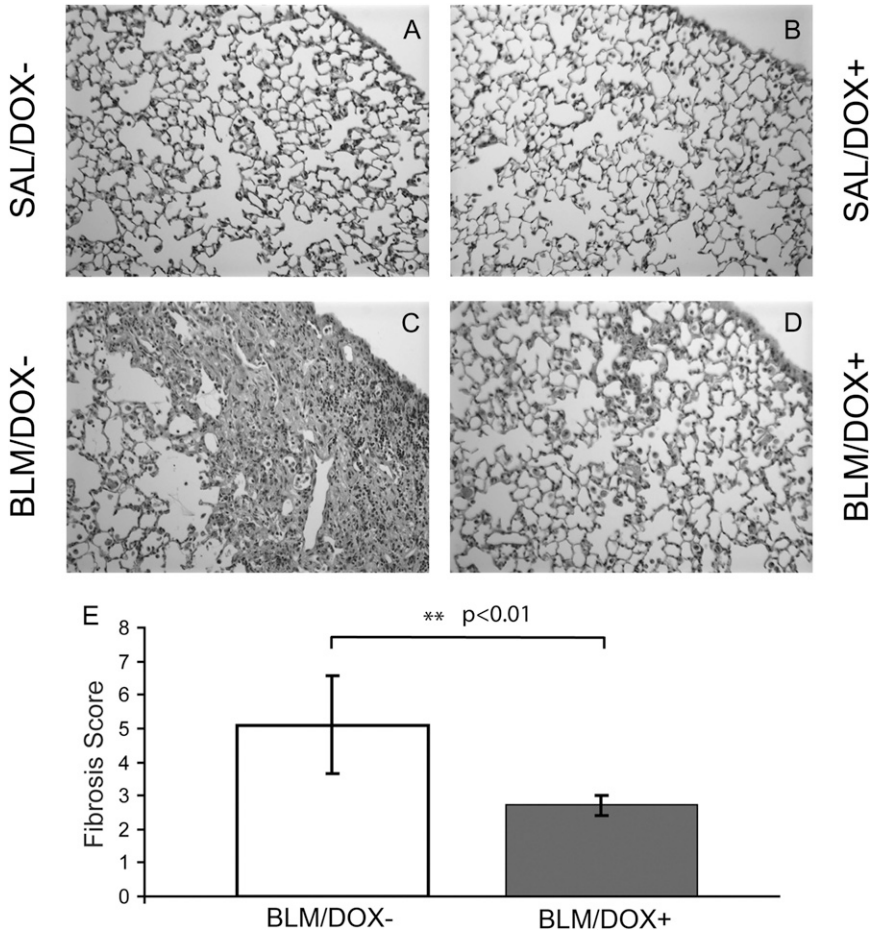

Figure 2. Histological analysis and quantitative fibrosis scoring of lung sections from adult *SP-C-rtTA*; *tet*(*O*)*Fgf10* mice. (*A–D*) Hematoxylin and eosin staining of 5-μm-thick lung sections (original magnification, ×10) of double-transgenic mice treated with (*A*) SAL/DOX$^-$, (*B*) SAL/DOX$^+$, (*C*) BLM/DOX$^-$, (*D*) BLM/DOX$^+$. BLM = bleomycin; DOX = doxycycline; SAL = saline. (*E*) Histological scoring of hematoxylin and eosin–stained sections of BLM/DOX$^+$ lungs (*shaded column*) showed suppression of bleomycin-induced fibrosis compared with the BLM/DOX$^-$ group (*open column*). Data are plotted as mean fibrosis score ± SD. A *P* value less than 0.01 was obtained between the BLM/DOX$^+$ and BLM/DOX$^-$ groups, using the *t* test (n = 3).

Bioactive TGF-β_1 BALF Levels Are Reduced in DOX-fed Bleomycin-treated Mice

In response to the administration of bleomycin an increase in the expression of *Tgfβ1* has been reported at the RNA and protein levels in the lung. TGF-β_1 is present in BALF in active and latent forms. The bioactive fraction of TGF-β_1 in BALF from the lungs of BLM-treated mice with or without DOX (n = 3 for each group) was measured in a well-established *PAI-1*-luciferase reporter assay on Days 3, 7, and 14. The BLM/DOX$^+$ group showed a significant twofold reduction in BALF levels of bioactive TGF-β_1 (Figure 5A; $P < 0.01$).

TGF-β receptors (TGF-βR1–3) activated by TGF-β can induce the phosphorylation of the downstream targets SMAD2 and SMAD3, thereby regulating transcriptional responses. In our analysis, there was a significant decrease in levels of both *Tgfβ1* and *Smad3* mRNAs in the lungs of mice from the BLM/DOX$^+$ group as compared with the BLM/DOX$^-$ group ($P < 0.01$, n = 4 in each group) (Figures 5C–5F). Lungs obtained 7 days after pump implantation from the BLM/DOX$^+$ group also exhibited a marked decrease in the phosphorylation of SMAD3 compared with the BLM/DOX$^-$ group (n = 3; Figure 5B). We also examined the expression of the integrin $\alpha_v\beta_6$, a major TGF-β activator in the lung (24). In lung sections of bleomycin-treated mice expression of integrin $\alpha_v\beta_6$ was observed at the 28-day time point in both BLM/DOX$^-$ and BLM/DOX$^+$ mice (Figures 6C and 6D). These results therefore indicate that the processing of latent to active TGF-β is not likely to have been significantly affected by *Fgf10* overexpression in BLM-treated mice.

An increase in matrix metalloproteinase (MMP) has been associated with alveolar destruction and progression of lung fibrosis (25, 26). Among the critical MMPs, MMP2 and MMP9 exhibit gelatinase activity that can be measured in a zymogram assay. Figure 6E shows a clear increase in both active and inactive MMP2 in the BALF from BLM/DOX$^-$ versus BLM/DOX$^+$ mice 7 and 14 days after pump implantation. Therefore our results show that in mice overexpressing *Fgf10,* metalloproteinase levels in BALF are drastically reduced.

Fgf10 Overexpression Leads to Increased Protection of Alveolar Epithelial Cells

To determine the cellular mechanism by which FGF10 mediates attenuation of lung fibrosis, global proliferation, and apoptosis in BLM/DOX$^+$, BLM/DOX$^-$, SAL/DOX$^+$, and SAL/DOX$^-$ lungs were analyzed on Days 14 and 28 after injury. Our results indicated a marked increase in apoptosis in BLM/DOX$^-$ as compared with SAL/DOX$^+$ or SAL/DOX$^-$ lungs, suggesting that bleomycin treatment triggered cell death (Figure 7G). Interestingly, the concomitant increase in proliferation in BLM/DOX$^-$ as compared with SAL/DOX$^+$ or SAL/DOX$^-$ lungs may suggest that mesenchymal cell proliferation is increased in BLM/DOX$^-$ lungs (Figure 7F). In addition, it is likely that an endogenous repair process is also occurring in BLM/DOX$^-$ lungs to replace the dying cells, as it has been reported that fibrosis eventually resolves in mice 6 to 10 weeks after bleomycin injury (27).

No significant difference in general proliferation and apoptosis was observed between BLM/DOX$^+$ and BLM/DOX$^-$

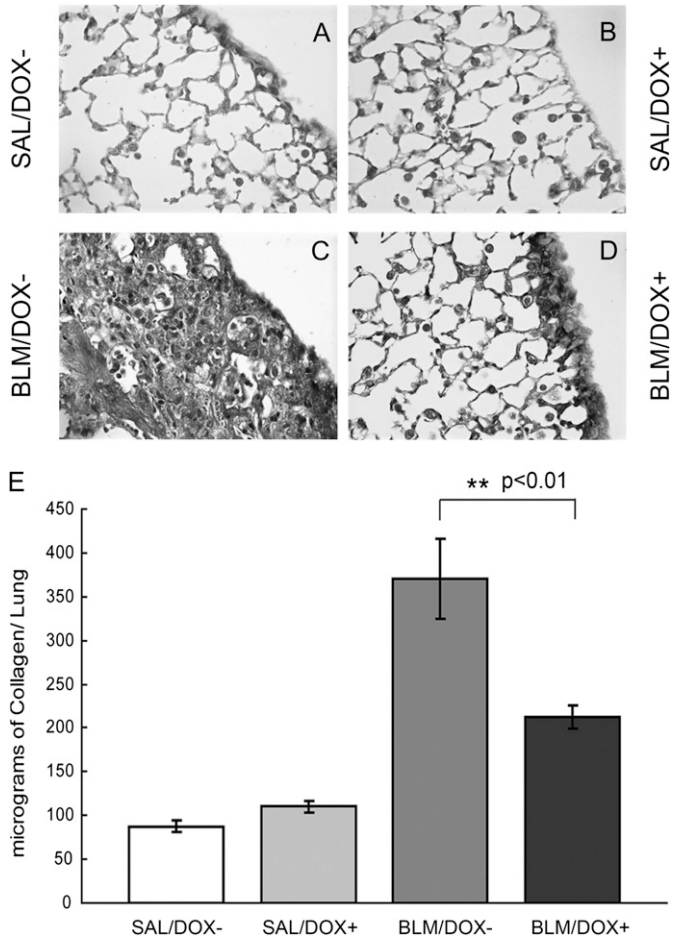

Figure 3. Collagen localization and quantification in adult *SP-C-rtTA*; *tet(O)Fgf10* mouse lungs. (*A–D*) Masson's trichrome staining of 5-μm-thick lung sections of double-transgenic mice treated with (*A*) SAL/DOX$^-$, (*B*) SAL/DOX$^+$, (*C*) BLM/DOX$^-$, or (*D*) BLM/DOX$^+$ (original magnification, ×16). BLM = bleomycin; DOX = doxycycline; SAL = saline. (*E*) Lung collagen was quantified by the Sircol assay. Each *column* represents the mean lung collagen content ± SD expressed as micrograms per right lung for each of the experimental groups (n = 3). Data were found significant by two-factor analysis of variance (at a critical value of 0.05) to compare between the four groups. Note the reduction in collagen content in bleomycin-treated mice from the BLM/DOX$^+$ group compared with the BLM/DOX$^-$ group.

lungs on Day 14 or 28 (Figures 7F and 7G). To specifically examine the outcome of epithelial cells in BLM/DOX$^+$ versus BLM/DOX$^-$ lungs, immunofluorescence staining for the alveolar epithelial cell marker surfactant protein (SP)-C was performed and indicated a significant increase in the number of SP-C–positive cells in BLM/DOX$^+$ versus BLM/DOX$^-$ lungs (Figures 7A–7E). To this end, our data suggested that FGF10 delivered during the acute inflammatory phase (Week 1) was acting in a protective manner on AEC2.

To further test this possibility, two independent approaches were taken. In the first approach, TUNEL and SP-C immunohistochemistry were performed on serial 5-μm-thick sections 28 days after the administration of bleomycin in BLM/DOX$^+$ mice (DOX was delivered during the first week) versus BLM/DOX$^-$ mice. The 28-day time point was chosen because the highest proliferation and apoptosis rates were noted in response to bleomycin and a significant difference in the number of SP-C–positive cells was observed in BLM/DOX$^+$ versus BLM/DOX$^-$ mice (Figures 7F and 7G). The percentage of SP-C and TUNEL double-positive cells compared with the total number of TUNEL-positive cells was 33.01 ± 9.97% in BLM/DOX$^-$ lungs versus 10.34 ± 2.83% in BLM/DOX$^+$ lungs (n = 3, $P < 0.05$). In addition, the percentage of SP-C and TUNEL double-positive cells versus the total number of SP-C–positive cells was equal to 5.62 ± 2.85% in BLM/DOX$^-$ lungs versus 1.43 ± 0.45% in BLM/DOX$^+$ lungs (n = 3, $P < 0.05$).

In a second approach, we isolated AEC2 from double-transgenic lungs in which exogenous *Fgf10* was induced 2 days before cell isolation, using rtTA expressed from the ubiquitous *Rosa26* promoter (15). Under our experimental conditions we were able to isolate a 95% pure SP-C–positive cell population (18). In double-transgenic mice not exposed to DOX, only 25.4 ± 12.3% of the seeded cells were alive on Day 2 whereas 49.9 ± 14.8% of the cells from lungs of double-transgenic mice exposed to DOX survived Day 2 after plating (Figure 8A). The difference between the number of cells in the DOX$^-$ group versus the DOX$^+$ group on Day 2 was statistically significant ($P < 0.05$). Cells isolated from the DOX$^-$ and DOX$^+$ groups were vimentin negative, cytokeratin positive, and SP-C positive (Figure 8B). Collectively, our data therefore demonstrate that FGF10 protects SP-C–positive cells from apoptosis.

Fgf10 Overexpression during the Fibrotic Phase Leads to Attenuation of Fibrosis

We finally examined whether overexpression of *Fgf10* during the fibrotic period (Day 7 through Day 14/Week 2 and Day 14 through Day 21/Week 3; Figure 9A) would similarly attenuate the extent of fibrosis. On Day 7, the beginning of Week 2, no sign of fibrosis and/or collagen deposition could be detected (data not shown). However, on Day 14, the beginning of Week 3, signs of fibrosis in the subpleural region and collagen deposition were visible (data not shown). Figures 9D and 9E indicate that *Fgf10* overexpression during Week 2 or Week 3 is indeed capable of decreasing fibrosis compared with BLM/DOX$^-$ lungs (Figure 9B) to a range similar to that observed when *Fgf10* is overexpressed during Week 1 (Figure 9C). Confirmation of these histological observations was obtained by measuring the Ashcroft Index score (n = 4, $P < 0.05$; Figure 9F) as well as collagen deposition evaluated on Day 28 after injury (n = 3, $P < 0.01$; Figure 9G). Our results therefore indicate that *Fgf10* overexpression during both the inflammatory and fibrotic phases reduces the extent of fibrosis.

DISCUSSION

Current Animal Models of Lung Fibrosis Do Not Comprehensively Reflect the Development of IPF Disease in Humans

Among the many mouse models of lung fibrosis, bleomycin delivered either intratracheally, intravenously, subcutaneously, or intranasally is best characterized (28). In our model, 2 weeks after subcutaneous bleomycin delivery the inflammatory response wanes and collagen deposition begins, marking the beginning of the fibrotic phase (21). A major difference between human IPF and bleomycin-induced lung fibrosis in mice is that in mice there is an increase in the accumulation of collagen for 4–6 weeks, which thereafter declines. Such a decline is not seen in humans; rather, a progressive decline in lung function and quality of life is encountered despite the administration of corticosteroids and antiinflammatory agents. One report shows that patients with IPF exhibit severe endoplasmic reticulum stress and apoptosis in alveolar type II cells (3).

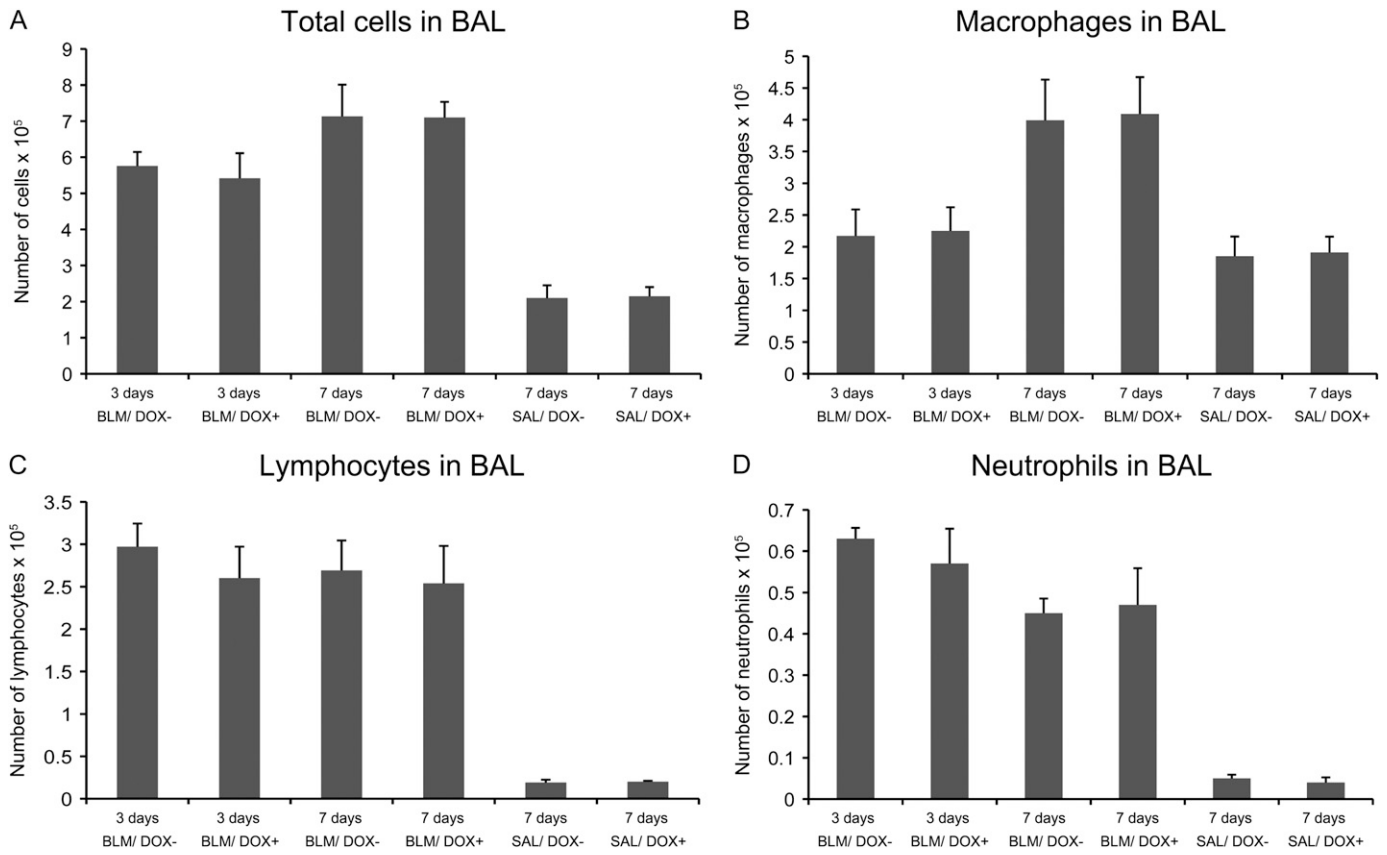

Figure 4. Differential cell counts in bleomycin-treated *SP-C-rtTA*; *tet*(*O*)*Fgf10* mice. Bronchoalveolar lavage (BAL) fluid was collected from *SP-C-rtTA*; *tet*(*O*)*Fgf10* mice treated with bleomycin for 3 and 7 days, respectively, to determine (*A*) the total cell count, as well as the differential cell counts of (*B*) macrophages, (*C*) lymphocytes, and (*D*) neutrophils. The experimental group was given a DOX diet (DOX^+) throughout this period and the control group was fed a normal diet. Analysis of variance showed no significant variation at either time point (for n = 4). DOX = doxycycline; SAL = saline.

Therefore growth factors capable of exerting protective effects on alveolar epithelial cells including the progenitor cell population represent prime candidates for therapeutic use. Among them, fibroblast growth factors (FGFs) acting on lung epithelial cells that express FGFR2b have raised significant interest. Our work focuses on the role of FGF10, a previously uncharacterized member of the family of FGFR2b ligands in the context of lung fibrosis.

FGFR2b Ligands and Their Role in Preventing Epithelial Injury and Promoting Lung Regeneration

The alveolar epithelium is composed of only two cell types: alveolar type I cells and alveolar type II cells (AEC2). AEC2 synthesize, store, and secrete pulmonary surfactant, which reduces surface tension and stabilizes alveolar units for efficient gas exchange. AEC2 are also the progenitor cells for type I cells, particularly during reepithelialization of the alveolus after lung injury. Several processes are involved in preventing lung injury and promoting lung repair and healing after injury. When type I cells are damaged, AEC2 divide, migrate, and spread along the denuded basement membrane surface; reform the epithelium; and finally differentiate into type I cells. AEC2 can modify the inflammatory response by secreting a variety of growth factors and cytokines. Regeneration of alveolar epithelial cells is thus one of the most important repair processes in many types of lung injury. AEC2 stimulation increases alveolar cell proliferation, surfactant production, and absorption of alveolar fluid. The interaction of soluble factors such as members of the FGF family and extracellular matrix components has a strong impact on alveolar type II cell proliferation.

FGF10 signaling in the epithelium via FGFR2b is essential for normal lung development. FGF10 is required early during the pseudo-glandular stage to control the survival, proliferation, and differentiation of the distal/alveolar epithelium. In the adult lung, FGFR2b signaling is dispensable for homeostasis but is again critical for the repair process induced by hyperoxia (9). Another structurally similar member of the FGF10 family, FGF7, is also required for normal lung alveologenesis and differentiation (29). Like FGF10, FGF7 also has the potential for therapeutic use that has been evaluated in disease models associated with damage to epithelial cells of the skin, digestive tract, and bladder. However, *Fgf7* null mice are viable with only subtle muscle regeneration and coat defects (30). The wound healing in these mice appears normal, suggesting that *Fgf10* is able to compensate for the loss of *Fgf7* in the repair process. Nevertheless, FGF7 and FGF10 have different affinities for the FGFR2b receptor (31) and display different biological activities *in vitro* (32). FGF7 acts mostly via FGFR2b whereas FGF10 acts via FGFR1b and FGFR2b (33).

Although there is abundant literature on the role of FGF7 in protecting against injury, there is little information about the role of FGF10 during the repair process. In pulmonary disease models intratracheal instillation of FGF7 prevents lung injury caused by radiation, hyperoxia, acids, as well as mechanical ventilation (34). It also causes proliferation of AEC type II and

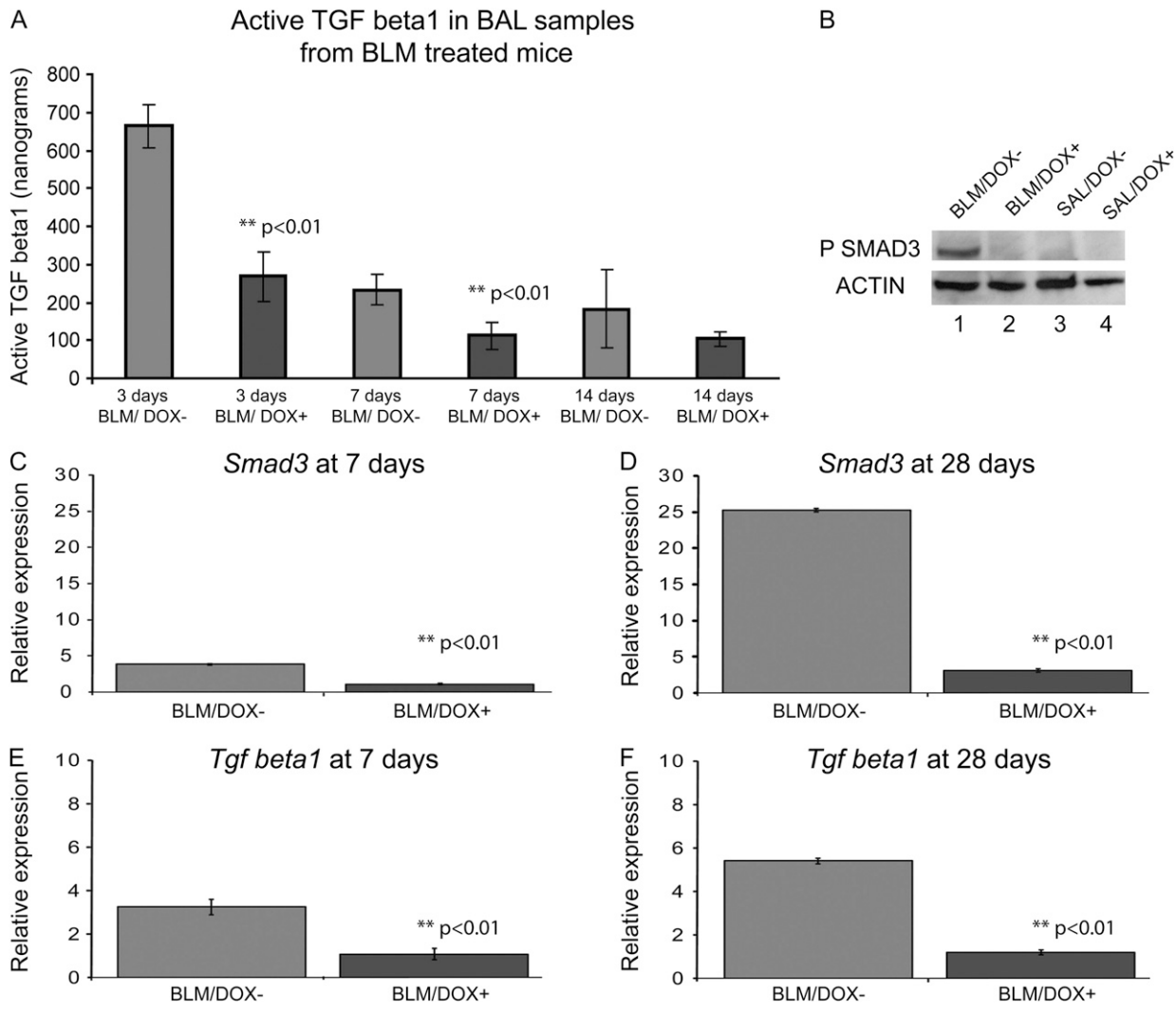

Figure 5. Quantification of endogenous bioactive transforming growth factor (TGF)-β_1 in bronchoalveolar lavage (BAL) fluid and molecular analysis of lung tissue collected from bleomycin (BLM)-treated *SP-C-rtTA; tet(O)Fgf10* mice. (*A*) The concentration of bioactive TGF-β_1 in BAL fluid obtained from the lungs of *SP-C-rtTA; tet(O)Fgf10* mice (n = 3) 3, 7, and 14 days after injury initiation is depicted as the mean ± SD of total nanograms obtained. A minimal twofold reduction of bioactive TGF-β_1 in doxycycline (DOX)-treated animals is observed at both time points. A *P* value less than 0.05 was obtained between BLM-treated DOX^+ versus DOX^- for each time point, using the *t* test. (*B–F*) Expression of protein and RNA in the lung lysates of *SP-C-rtTA; tet(O)Fgf10* mice at 7 days. (*B*) Expression of phospho-SMAD3 protein in *SP-C-rtTA; tet(O)Fgf10* mice treated with the following: lane 1, BLM/DOX^-; lane 2, BLM/DOX^+; lane 3, SAL/DOX^-; lane 4, SAL/DOX^+ at 7 days after injury initiation. A clear band for phospho-SMAD3 is observed for the BLM/DOX^- group (lane 1), which is not visible for any of the other groups. (*C–F*) Comparisons are made between the BLM/DOX^+ and BLM/DOX^- groups of mice. There is about a sixfold increase in *Tgfβ1* and a threefold increase in *Smad3* RNA by real-time analysis between the two groups of bleomycin-treated mice 28 days after pump implantation.

bronchial cells. The role of FGF7 in preventing lung fibrosis has also been reported (35), in which BLM was intratracheally injected to induce acute fibrosis in rats. FGF7 pretreatment 72 and 48 hours before BLM yielded a significant reduction in neutrophil levels as well as minimal to no visible lung injury. Another, similar study reported an increase in survival rates of rats that were given BLM intratracheally and then exposed to BLM alone or to BLM and irradiation (36). In addition, a double intratracheal instillation of FGF7 in rats both 48 hours before as well as 24 hours after BLM treatment resulted in prevention of BLM-induced fibrosis (37). FGF7 is also effective in BLM lung injury models when administered either intravenously or by the intratracheal method (38). In these studies it was speculated that FGF7 was able to ameliorate lung injury by increasing lung surfactant protein production, thereby promoting the maintenance of alveolar epithelial integrity. However, none of these experimental approaches using FGF7 recombinant proteins was capable of significantly attenuating fibrosis when the growth factor was administered during the fibrotic phase. One of the questions raised by these negative data concerns whether type II progenitor cells have access to the growth factor as the lung becomes fibrotic. To design and improve existing therapies against fibrosis, it is important to identify whether epithelial progenitor cells present in the fibrotic lungs can still be stimulated to attenuate lung fibrosis. Herein we focused on the previously unknown role of FGF10 in lung fibrosis. We used genetically engineered mice to allow inducible expression of *Fgf10* directly in type II cells. We first tested whether FGF10 would provide injury prevention when delivered during the inflammatory phase in a bleomycin-induced mouse model of lung fibrosis. We also expanded our study to analyze the potential consequences of *Fgf10* over-

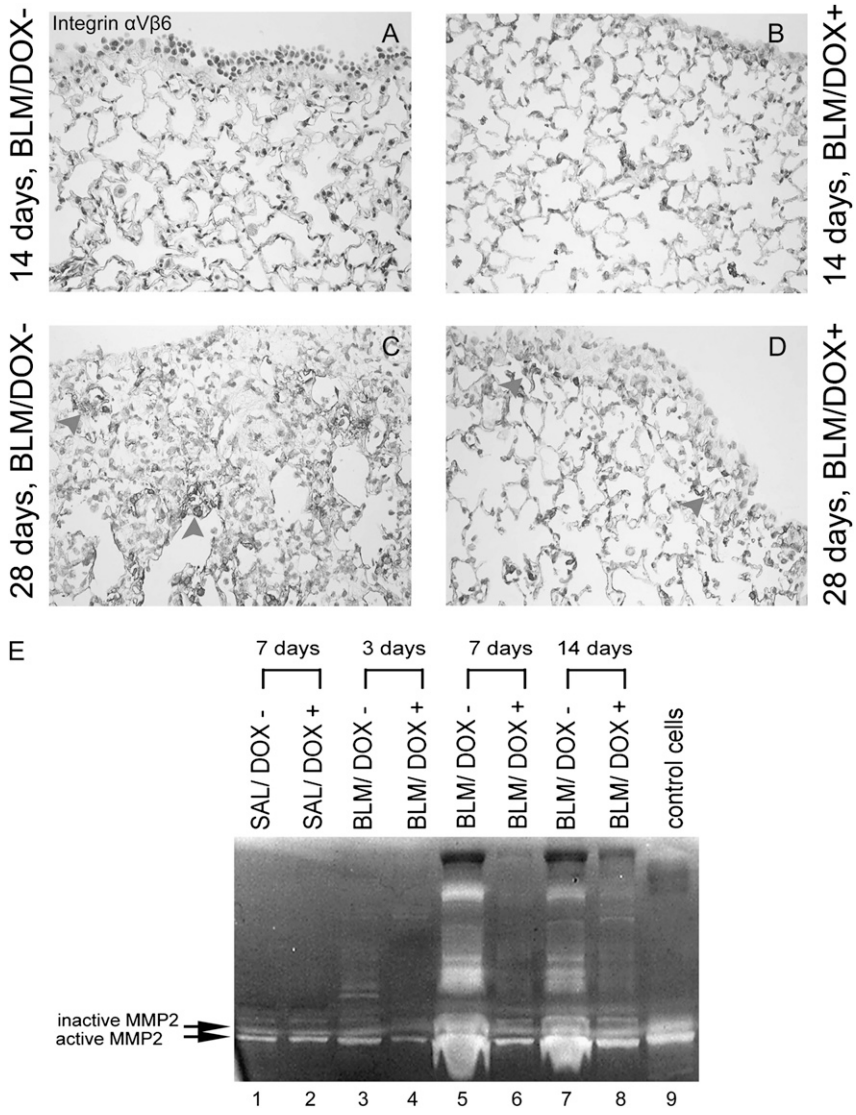

Figure 6. Detection of $\alpha_v\beta_6$ in lung sections (*A–D*) and matrix metalloproteinase (MMP) activity (*E*) in bronchoalveolar lavage obtained from bleomycin-treated *SP-C-rtTA*; *tet*(*O*)*Fgf10* mice. (*A–D*) $\alpha_v\beta_6$ expression in *SP-C-rtTA*; *tet*(*O*)*Fgf10* mice at the 14- and 28-day time points. At the 14-day time point no difference was obtained between the BLM/DOX$^-$ and BLM/DOX$^+$ groups. At the 28-day time point, we observed staining for $\alpha_v\beta_6$ in fibrotic regions of the lungs in both the BLM/DOX$^-$ and BLM/DOX$^+$ groups. At the 28-day time points, we also observed staining for $\alpha_v\beta_6$ in fibrotic regions of lungs in both the BLM/DOX$^-$ and BLM/DOX$^+$ groups (*arrowheads*) (*E*) On Days 7 and 14 after pump implantation, BAL fluid from bleomycin-treated mice fed a normal diet exhibited increased levels of MMP2 (both active and inactive) as compared with BAL fluid from bleomycin mice fed a doxycycline (DOX$^+$) diet. Lanes 1 and 2, BAL fluid from mice treated with saline (SAL), receiving normal chow (DOX$^-$) or chow containing doxycycline (DOX$^+$) and killed 7 days after pump implantation; lanes 3–8, BAL fluid from bleomycin (BLM)-treated mice fed either normal chow (DOX$^-$) or chow containing doxycycline (DOX$^+$) and killed 3, 7, and 14 days after pump implantation; lane 9, conditioned medium from control NIH/3T3 cells positive for both the active and the inactive forms of MMP2.

expression by type II cells during the most clinically relevant fibrotic phase.

Regulatory T Cells Are Increased on *Fgf10* Overexpression during the Bleomycin-induced Inflammatory Phase

Bleomycin-induced lung fibrosis can be divided into two phases (39). In the inflammatory phase chemoattractant agents derived from the injured lung tissue bring about the initial recruitment of inflammatory cells into the alveolar spaces. Increased permeability of the pulmonary epithelium and the endothelium is a prominent feature and fibrin is formed in the alveolar lumen because of local activation of the coagulation system. TGF-β is one such chemotactic factor that activates inflammatory macrophages and monocytes to release a number of cytokines such as platelet-derived growth factor, IL-1β, and tumor necrosis factor-α. In our model, the switch from the inflammatory phase to fibrotic phase occurs about 9 days after the start of injury. Our initial experiments used the preventive treatment approach to overexpress *Fgf10* simultaneously (Week 1) with the induction of bleomycin injury.

During the fibrotic phase, TGF-β_1 acts as a potent promoter of extracellular matrix production. In our *SP-C-rtTA*; *tet*(*O*)*Fgf10* BLM/DOX$^+$ mice, the reduction in *Tgfβ1* on RNA and protein levels, 7 and 28 days postinjury, may largely explain the lowered collagen deposition observed in the 28-day lung sections from these mice as compared with the BLM/DOX$^-$ mice. In studies in which FGF7 administration ameliorated fibrosis in BLM-induced models, a reduction in inflammation levels was also reported. In our experiments, we observed a reduction in fibrosis without a significant reduction in total as well as differential inflammatory cell counts in the BALF. However, we observed a significant increase in CD4$^+$CD25$^+$Foxp3$^+$ T-regulatory cells in the BAL of BLM/DOX$^+$ versus BMLM/DOX$^-$ mice. This subpopulation of T cells has been shown to be reduced in the BALF of patients with IPF (23) and may therefore contribute to the development of lung fibrosis. How FGF10 is capable of triggering the increase in Treg cells will be explored in further studies.

Thus, *Fgf10* overexpression attenuates bleomycin-induced lung fibrosis through a potential suppression of inflammation involving the maintenance and or recruitment of the Treg population as well as reduction of TGF-β expression and activity. Interestingly, bleomycin delivery in *Smad3* null mice leads to reduction of fibrosis without affecting inflammation (40). The regulation of Treg cells in the BAL of this mouse model under normal and fibrotic conditions is still unknown. This would indicate that inflammation and fibrosis are not always directly linked and this may explain why antiinflammatory treatments in humans with IPF are ineffective.

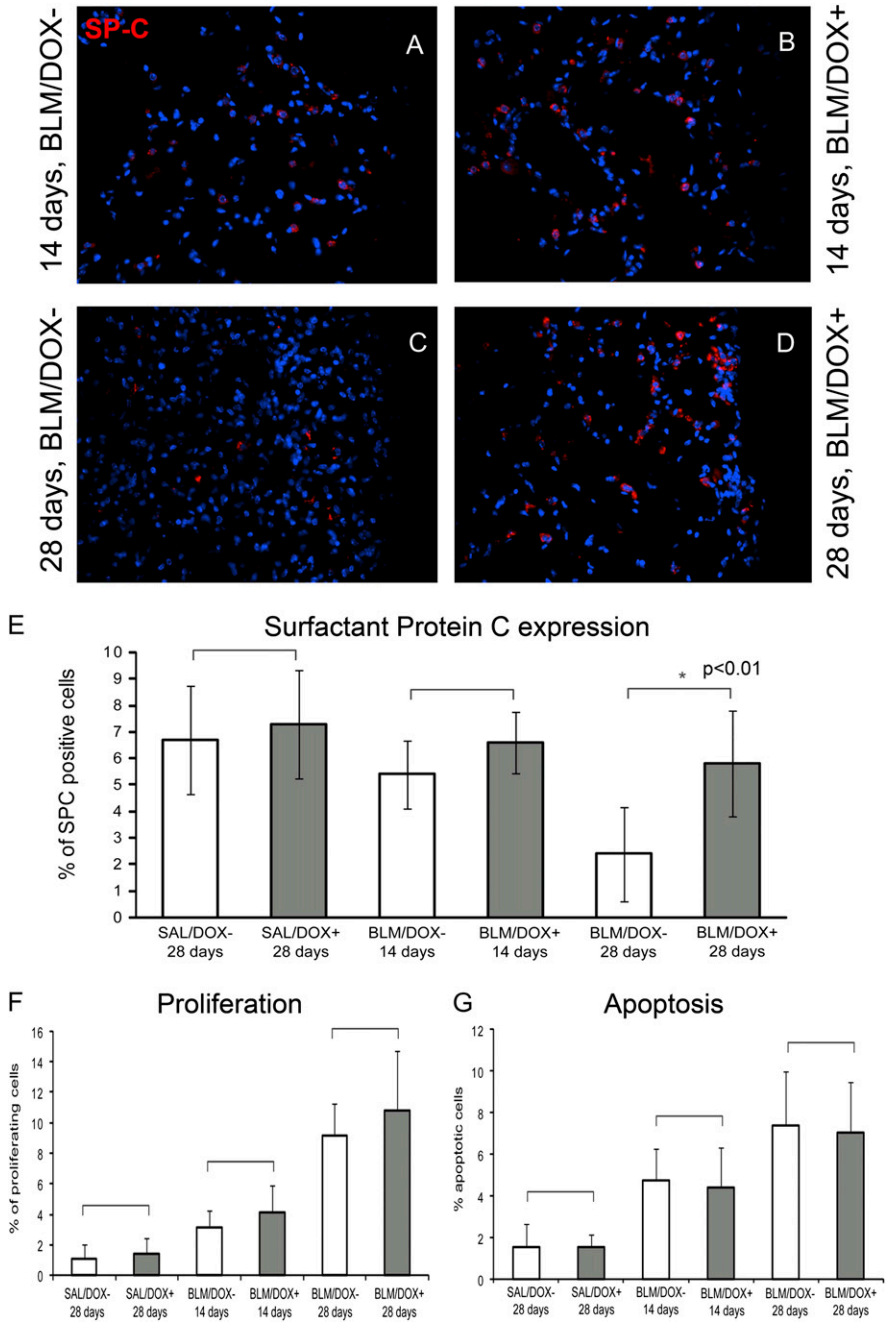

Figure 7. Immunohistochemical analysis of sections from bleomycin-treated animals. (*A–D*) Surfactant protein C expression in bleomycin-treated mice at 14-day (*A* and *B*) and 28-day time points (*C* and *D*) shows that mice fed a doxycycline $(DOX)^+$ diet exhibit more SP-C–positive cells. This is further quantified as the percentage of SP-C–positive cells in (*E*). Note the reduction in the percentage of SP-C–positive cells in the BLM/DOX^- group at the 28-day time point. The difference in percentage of positive cells is significant between the BLM/DOX^- and BLM/DOX^+ groups at the 28-day time point (n = 5 fields of observation at a magnification of ×40; $P < 0.05$ by *t* test). (*F* and *G*) Quantification of proliferation and apoptosis in sections from these mice reveals no significant difference between the respective groups (marked by *brackets*) as determined by *t* test (n = 5 fields of observation at a magnification of ×40 in each case). Data are plotted as mean fibrosis score ± SD.

The distinctive feature of IPF is the predominance of fibroblastic foci. Whether inflammation is required for the progression of fibrosis has been debated (41, 42). *Tgfβ* knockout mice demonstrate severe inflammatory reactions in various organs, including the lung. TGF-β overexpression results in extensive fibrosis in mouse or rat lung without any preceding major inflammation (43). In contrast, overexpression of IL-1β in rat lung induces severe tissue destruction, inflammation, and subsequently progressive fibrosis (44). However, when IL-1β is administered to *Smad3* null mice, both tissue injury and the inflammatory response are present, but the mutant mice do not progress to the fibrotic phenotype (45). Hence IL-1β is linked to fibrosis through TGF-β and SMAD3 signaling but not directly through increased inflammation (6, 45, 46).

Our results indicate a reduction in active MMP2 in the BAL samples from BLM-treated mice that are overexpressing *Fgf10* compared with the BLM/DOX^- group (Figure 6). In addition to MMP2, MMP12 is another matrix metalloproteinase known to play an important role in bleomycin-related tissue pathogenesis. MMP12 is stimulated and activated by TGF-β_1 via Bid and Bax mechanisms (47). Potential reduction in MMP12, in addition of MMP2, could therefore also account for the attenuation of fibrosis in the BLM/DOX^+ group.

Thus *Fgf10* overexpression during the inflammatory phase likely leads to attenuation of fibrosis by increasing the Treg subpopulation and preventing an increase in TGF-β_1 levels both at the RNA and protein levels. This makes the use of this growth factor extremely attractive as a candidate to ameliorate diseases due to increased TGF-β_1 expression in the lung. Clinical trials aiming to neutralize TGF-β_1 activity with blocking antibodies or small inhibitors are currently underway. Our work indicates that in addition to these approaches, FGF10

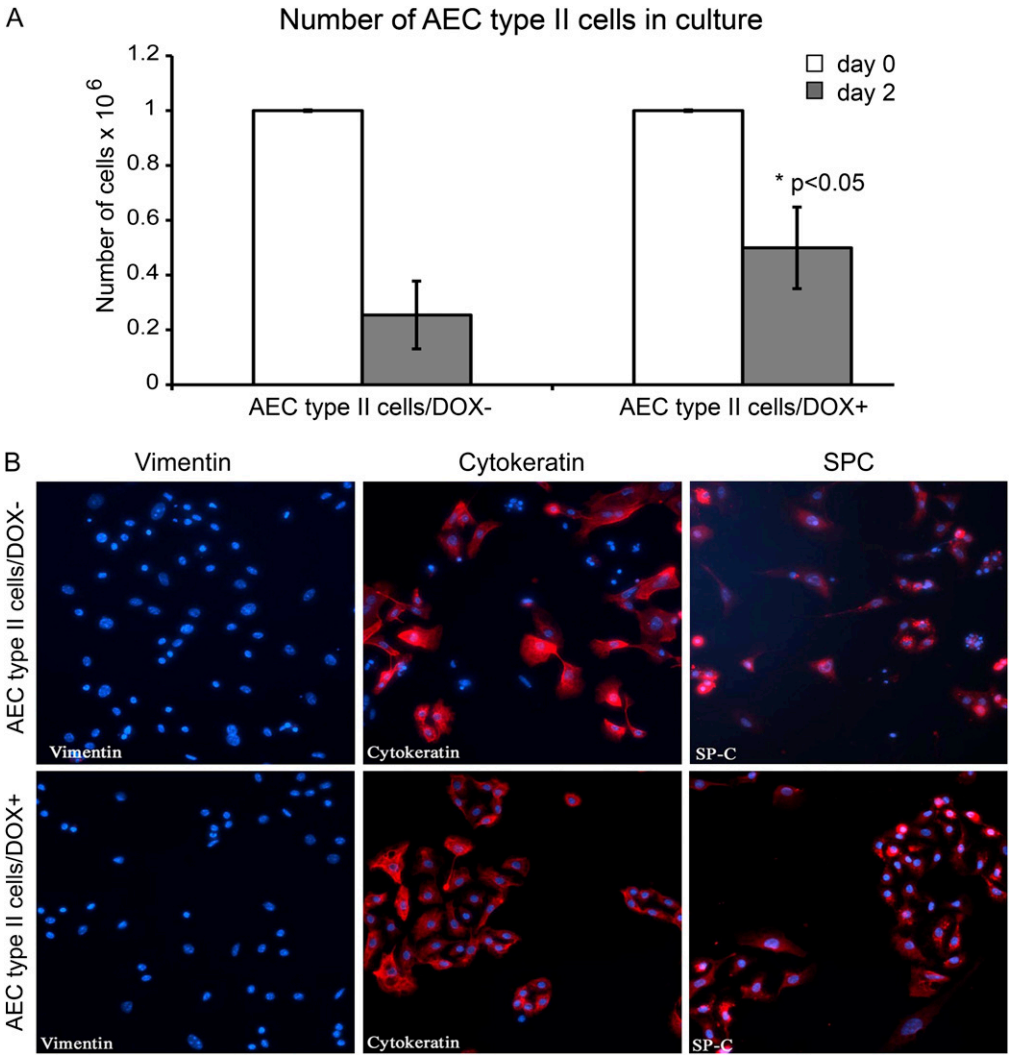

Figure 8. Survival of isolated alveolar type II cells expressing *Fgf10*. (*A*) One million alveolar type II cells (AEC2) isolated from mouse lungs were plated on the day of isolation (Day 0) and were counted 2 days later. The number of cells on Day 2 after isolation revealed that twice as many AEC2 survived when *Fgf10* was overexpressed by adding doxycycline to the medium (DOX^+) as compared with DOX^- medium (n = 4). (*B*) Immunohistochemical staining revealed that the isolated AEC2/DOX^- and AEC2/DOX^+ cells were vimentin negative, cytokeratin positive, and surfactant protein (SP)-C positive 2 days (Day 2) after isolation.

could also be used to reduce the expression of bioactive TGF-β_1.

Fgf10 Overexpression during the Fibrotic Phase Leads to Attenuation of Lung Fibrosis

The most surprising and clinically promising data in this report indicate that expression of *Fgf10* directly by AEC2 during the fibrotic phase (Weeks 2 and 3) leads to significant attenuation of fibrosis. This suggests that type II epithelial progenitor cells present in the fibrotic lung are still capable of responding to FGF10 and that better delivery of the growth factor to the alveolar space may attenuate the progression of lung fibrosis in humans or in mouse models. The mechanism of action of FGF10 on epithelial progenitors has been previously reported. FGF10 is known to be a potent chemoattractant for the distal lung epithelium (48). It has been shown to regulate prenatal differentiation and acts, at least during the early pseudo-glandular phase of lung development, as a survival and proliferative factor for distal epithelial progenitor cells. It has also been reported that the pancreas of *Fgf10* null embryos is depleted of epithelial progenitor cells, leading to arrest of growth and differentiation of the epithelium (49). *Fgf10* overexpression, on the other hand, is reported to lead to an expansion of progenitor cells and attenuation of differentiation (50). A similar function is seen in the gastrointestinal tract, as *Fgf10* null mice exhibit a decrease in dividing progenitor cells whereas ectopic overexpression leads to attenuation of differentiation in a lineage-specific manner. We have previously shown that *Fgf10* gene dosage in the lungs is critical for distal epithelial progenitor cell amplification (7). Thus, *Fgf10* overexpression in the BLM/DOX^+ group might maintain the survival of epithelial progenitor cells located in the respiratory airways, thereby being responsible for maintaining the integrity of the AECs during fibrotic lung injury. In harmony with this hypothesis, on *Fgf10* overexpression, we observed an increase in the expression of SP-C as a marker for AEC2 as well as a decreased number of SP-C/TUNEL double-positive cells and increased survival when type II cells were isolated and cultured *in vitro*. It is unknown how restoring epithelial integrity mediates the decrease in expression of TGF-β_1 both at the RNA and protein levels. It is clear, however, that alveolar epithelial cells have the capacity to secrete products known to inhibit fibroblast proliferation and collagen synthesis such as prostaglandin E_2 (5). Interestingly, intratracheal administration of isolated alveolar type II cells during the fibrotic phase has also been shown to significantly attenuate bleomycin-induced lung fibrosis (6). In the future it will be important to identify the secreted products that attenuate fibrosis. It is likely that the synthesis of these products will be increased on stimulation with FGFR2b ligands.

In conclusion, the studies reported here have shown that BLM-induced lung fibrosis is attenuated by *Fgf10* overexpression not only during the inflammatory phase but also during the more clinically relevant fibrotic phase. Our results can there-

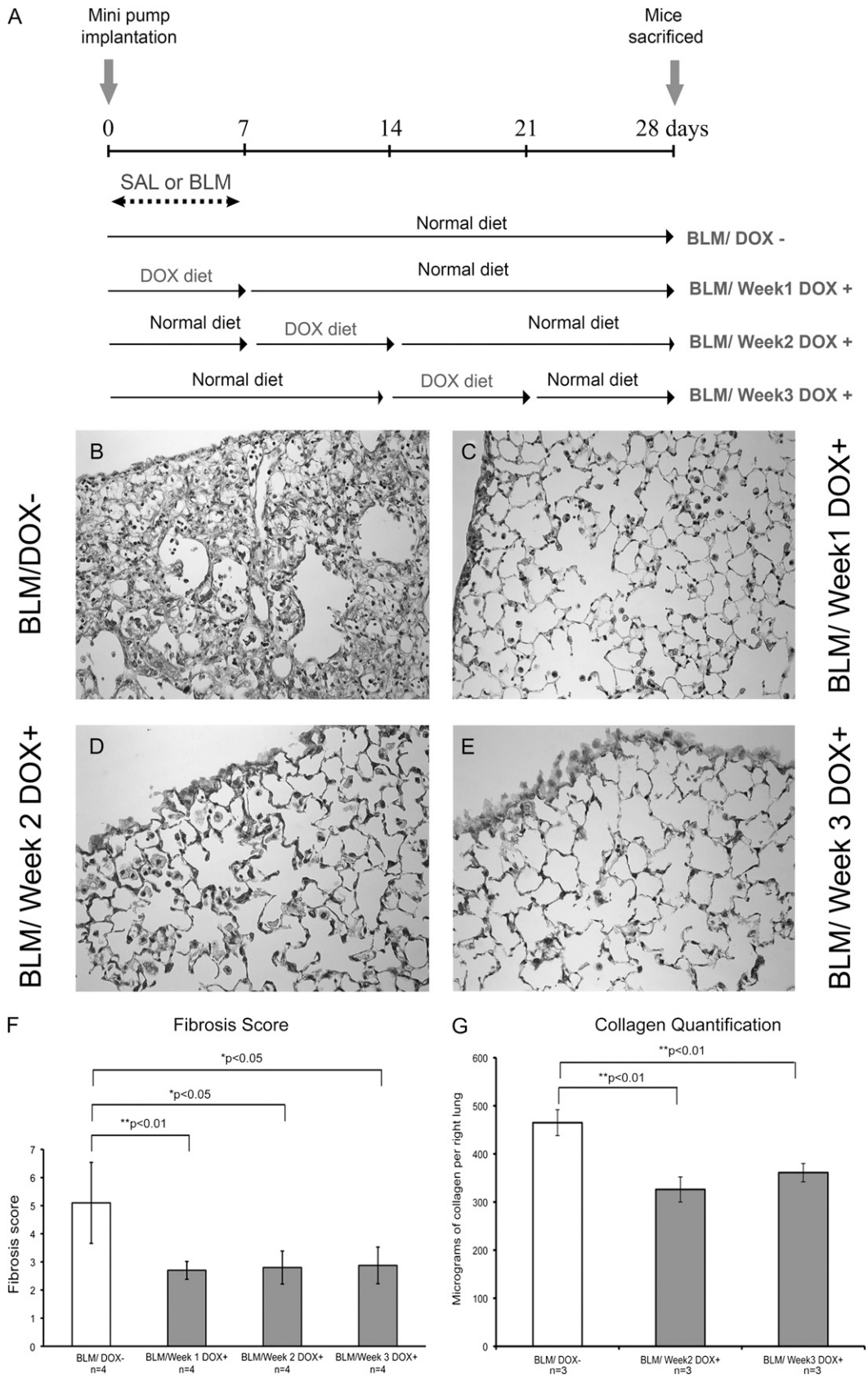

Figure 9. Overexpression of *Fgf10* during the second and third weeks after surgery leads to attenuation of lung fibrosis. (*A*) Experimental scheme depicting the time of doxycycline treatment of *SP-C-rtTA*; *tet(O)Fgf10* mice. Depending on whether the DOX$^+$ diet was given 1, 2, or 3 weeks after pump implantation, the mice were categorized as BLM/Week 1 DOX$^+$, BLM/Week 2 DOX$^+$, and BLM/Week 3 DOX$^+$ respectively. (*B–E*) Collagen localization and quantification in adult *SP-C-rtTA*; *tet(O)Fgf10* mouse lungs. Masson's trichrome staining of 5-μm-thick lung sections of bleomycin-treated double-transgenic mice overexpressing FGF10 in Week 1 (*C*), Week 2 (*D*) and Week 3 (*E*). Control BLM/DOX$^-$ (*B*) sections show a large amount of collagen in the lung. (*F*) Histological scoring of hematoxylin and eosin–stained sections of BLM/DOX$^+$ lungs (*shaded columns*) showed a suppression of bleomycin-induced fibrosis as compared with the BLM/DOX$^-$ group (*open column*). Data are plotted as mean fibrosis score ± SD. (*G*) Lung collagen was quantified by the Sircol assay. Each *column* represents the mean lung collagen content ± SD, expressed as micrograms per right lung for each of the experimental groups (n = 3).

fore be used as the rationale to improve the existing treatments for pulmonary fibrosis by devising improved delivery of FGFR2b ligands at the level of endogenous type II progenitor cells.

Conflict of Interest Statement: None of the authors has a financial relationship with a commercial entity that has an interest in the subject of this manuscript.

Acknowledgment: The authors thank Clarence Wigfall for help in editing the manuscript.

References

1. Kim DS, Collard HR, King TE Jr. Classification and natural history of the idiopathic interstitial pneumonias. *Proc Am Thorac Soc* 2006;3: 285–292.
2. American Thoracic Society, European Respiratory Society. Idiopathic pulmonary fibrosis: diagnosis and treatment [international consensus statement]. *Am J Respir Crit Care Med* 2000;161:646–664.
3. Korfei M, Ruppert C, Mahavadi P, Henneke I, Markart P, Koch M, Lang G, Fink L, Bohle RM, Seeger W, *et al.* Epithelial endoplasmic reticulum stress and apoptosis in sporadic idiopathic pulmonary fibrosis. *Am J Respir Crit Care Med* 2008;178:838–846.
4. Thannickal VJ, Toews GB, White ES, Lynch JP III, Martinez FJ. Mechanisms of pulmonary fibrosis. *Annu Rev Med* 2004;55:395–417.
5. Young L, Adamson IY. Epithelial–fibroblast interactions in bleomycin-induced lung injury and repair. *Environ Health Perspect* 1993;101:56–61.
6. Serrano-Mollar A, Nacher M, Gay-Jordi G, Closa D, Xaubet A, Bulbena O. Intratracheal transplantation of alveolar type II cells reverses bleomycin-induced lung fibrosis. *Am J Respir Crit Care Med* 2007;176:1261–1268.
7. Ramasamy SK, Mailleux AA, Gupte VV, Mata F, Sala FG, Veltmaat JM, Del Moral PM, De Langhe S, Parsa S, Kelly LK, *et al. Fgf10* dosage is critical for the amplification of epithelial cell progenitors and for the formation of multiple mesenchymal lineages during lung development. *Dev Biol* 2007;307:237–247.
8. Sekine K, Ohuchi H, Fujiwara M, Yamasaki M, Yoshizawa T, Sato T, Yagishita N, Matsui D, Koga Y, Itoh N, *et al.* Fgf10 is essential for limb and lung formation. *Nat Genet* 1999;21:138–141.
9. Hokuto I, Perl AK, Whitsett JA. FGF signaling is required for pulmonary homeostasis following hyperoxia. *Am J Physiol Lung Cell Mol Physiol* 2004;286:L580–L587.
10. Marchand-Adam S, Plantier L, Bernuau D, Legrand A, Cohen M, Marchal J, Soler P, Leseche G, Mal H, Aubier M, *et al.* Keratinocyte growth factor expression by fibroblasts in pulmonary fibrosis: poor response to interleukin-1β. *Am J Respir Cell Mol Biol* 2005;32:470–477.
11. Igarashi M, Finch PW, Aaronson SA. Characterization of recombinant human fibroblast growth factor (FGF)-10 reveals functional similarities with keratinocyte growth factor (FGF-7). *J Biol Chem* 1998;273: 13230–13235.
12. Jimenez PA, Rampy MA. Keratinocyte growth factor-2 accelerates wound healing in incisional wounds. *J Surg Res* 1999;81:238–242.
13. Upadhyay D, Correa-Meyer E, Sznajder JI, Kamp DW. FGF-10 prevents mechanical stretch–induced alveolar epithelial cell DNA damage via MAPK activation. *Am J Physiol Lung Cell Mol Physiol* 2003;284:L350–L359.
14. Clark JC, Tichelaar JW, Wert SE, Itoh N, Perl AK, Stahlman MT, Whitsett JA. FGF-10 disrupts lung morphogenesis and causes pulmonary adenomas *in vivo*. *Am J Physiol Lung Cell Mol Physiol* 2001; 280:L705–L715.
15. Parsa S, Ramasamy SK, De Langhe S, Gupte VV, Haigh JJ, Medina D, Bellusci S. Terminal end bud maintenance in mammary gland is dependent upon FGFR2b signaling. *Dev Biol* 2008;317:121–131.
16. Weinreb PH, Simon KJ, Rayhorn P, Yang WJ, Leone DR, Dolinski BM, Pearse BR, Yokota Y, Kawakatsu H, Atakilit A, *et al.* Function-blocking integrin $\alpha_v\beta_6$ monoclonal antibodies: distinct ligand-mimetic and nonligand-mimetic classes. *J Biol Chem* 2004;279: 17875–17887.
17. Ashcroft T, Simpson JM, Timbrell V. Simple method of estimating severity of pulmonary fibrosis on a numerical scale. *J Clin Pathol* 1988;41:467–470.
18. Lee J, Reddy R, Barsky L, Weinberg K, Driscoll B. Contribution of proliferation and DNA damage repair to alveolar epithelial type 2 cell recovery from hyperoxia. *Am J Physiol Lung Cell Mol Physiol* 2006;290:L685–L694.
19. Yoshimura S, Nishimura Y, Nishiuma T, Yamashita T, Kobayashi K, Yokoyama M. Overexpression of nitric oxide synthase by the endothelium attenuates bleomycin-induced lung fibrosis and impairs MMP-9/TIMP-1 balance. *Respirology* 2006;11:546–556.
20. Jules-Elysee K, White DA. Bleomycin-induced pulmonary toxicity. *Clin Chest Med* 1990;11:1–20.
21. Chung MP, Monick MM, Hamzeh NY, Butler NS, Powers LS, Hunninghake GW. Role of repeated lung injury and genetic background in bleomycin-induced fibrosis. *Am J Respir Cell Mol Biol* 2003;29: 375–380.
22. von Boehmer H. Notch in lymphopoiesis and T cell polarization. *Nat Immunol* 2005;6:641–642.
23. Kotsianidis I, Nakou E, Bouchliou I, Tzouvelekis A, Spanoudakis E, Steiropoulos P, Sotiriou I, Aidinis V, Margaritis D, Tsatalas C, Bouros D. Global impairment of $CD4^+CD25^+FOXP3^+$ regulatory T cells in idiopathic pulmonary fibrosis. *Am J Respir Crit Care Med* 2009;179:1121–1130.
24. Munger JS, Huang X, Kawakatsu H, Griffiths MJ, Dalton SL, Wu J, Pittet JF, Kaminski N, Garat C, Matthay MA, *et al.* The integrin $\alpha_v\beta_6$ binds and activates latent TGF-β_1: a mechanism for regulating pulmonary inflammation and fibrosis. *Cell* 1999;96:319–328.
25. Gueders MM, Foidart JM, Noel A, Cataldo DD. Matrix metalloproteinases (MMPs) and tissue inhibitors of MMPs in the respiratory tract: potential implications in asthma and other lung diseases. *Eur J Pharmacol* 2006;533:133–144.
26. Ito I, Nagai S, Handa T, Muro S, Hirai T, Tsukino M, Mishima M. Matrix metalloproteinase-9 promoter polymorphism associated with upper lung dominant emphysema. *Am J Respir Crit Care Med* 2005; 172:1378–1382.
27. Miyazaki H, Kuwano K, Yoshida K, Maeyama T, Yoshimi M, Fujita M, Hagimoto N, Yoshida R, Nakanishi Y. The perforin mediated apoptotic pathway in lung injury and fibrosis. *J Clin Pathol* 2004;57: 1292–1298.
28. Moore BB, Hogaboam CM. Murine models of pulmonary fibrosis. *Am J Physiol Lung Cell Mol Physiol* 2008;294:L152–L160.
29. Post M, Souza P, Liu J, Tseu I, Wang J, Kuliszewski M, Tanswell AK. Keratinocyte growth factor and its receptor are involved in regulating early lung branching. *Development* 1996;122:3107–3115.
30. Guo L, Degenstein L, Fuchs E. Keratinocyte growth factor is required for hair development but not for wound healing. *Genes Dev* 1996;10: 165–175.
31. Ohuchi H, Hori Y, Yamasaki M, Harada H, Sekine K, Kato S, Itoh N. FGF10 acts as a major ligand for FGF receptor 2 IIIb in mouse multi-organ development. *Biochem Biophys Res Commun* 2000;277:643–649.
32. Bellusci S, Grindley J, Emoto H, Itoh N, Hogan BL. Fibroblast growth factor 10 (FGF10) and branching morphogenesis in the embryonic mouse lung. *Development* 1997;124:4867–4878.
33. Zhang X, Ibrahimi OA, Olsen SK, Umemori H, Mohammadi M, Ornitz DM. Receptor specificity of the fibroblast growth factor family: the complete mammalian FGF family. *J Biol Chem* 2006;281:15694–15700.
34. Yano T, Deterding RR, Simonet WS, Shannon JM, Mason RJ. Keratinocyte growth factor reduces lung damage due to acid instillation in rats. *Am J Respir Cell Mol Biol* 1996;15:433–442.
35. Deterding RR, Havill AM, Yano T, Middleton SC, Jacoby CR, Shannon JM, Simonet WS, Mason RJ. Prevention of bleomycin-induced lung injury in rats by keratinocyte growth factor. *Proc Assoc Am Physicians* 1997;109:254–268.
36. Yi ES, Williams ST, Lee H, Malicki DM, Chin EM, Yin S, Tarpley J, Ulich TR. Keratinocyte growth factor ameliorates radiation- and bleomycin-induced lung injury and mortality. *Am J Pathol* 1996;149: 1963–1970.
37. Sugahara K, Iyama K, Kuroda MJ, Sano K. Double intratracheal instillation of keratinocyte growth factor prevents bleomycin-induced lung fibrosis in rats. *J Pathol* 1998;186:90–98.
38. Guo J, Yi ES, Havill AM, Sarosi I, Whitcomb L, Yin S, Middleton SC, Piguet P, Ulich TR. Intravenous keratinocyte growth factor protects against experimental pulmonary injury. *Am J Physiol* 1998;275:L800–L805.
39. Chaudhary NI, Schnapp A, Park JE. Pharmacologic differentiation of inflammation and fibrosis in the rat bleomycin model. *Am J Respir Crit Care Med* 2006;173:769–776.
40. Zhao Y, Geverd DA. Regulation of SMAD3 expression in bleomycin-induced pulmonary fibrosis: a negative feedback loop of TGF-β signaling. *Biochem Biophys Res Commun* 2002;294:319–323.

41. Gauldie J, Kolb M, Sime PJ. A new direction in the pathogenesis of idiopathic pulmonary fibrosis? *Respir Res* 2002;3:1.
42. Strieter RM. Inflammatory mechanisms are not a minor component of the pathogenesis of idiopathic pulmonary fibrosis. *Am J Respir Crit Care Med* 2002;165:1206–1207.
43. Pogach MS, Cao Y, Millien G, Ramirez MI, Williams MC. Key developmental regulators change during hyperoxia-induced injury and recovery in adult mouse lung. *J Cell Biochem* 2007;100:1415–1429.
44. Kolb M, Margetts PJ, Anthony DC, Pitossi F, Gauldie J. Transient expression of IL-1β induces acute lung injury and chronic repair leading to pulmonary fibrosis. *J Clin Invest* 2001;107:1529–1536.
45. Bonniaud P, Kolb M, Galt T, Robertson J, Robbins C, Stampfli M, Lavery C, Margetts PJ, Roberts AB, Gauldie J. Smad3 null mice develop airspace enlargement and are resistant to TGF-β–mediated pulmonary fibrosis. *J Immunol* 2004;173:2099–2108.
46. Bonniaud P, Margetts PJ, Ask K, Flanders K, Gauldie J, Kolb M. TGF-β and *smad3* signaling link inflammation to chronic fibrogenesis. *J Immunol* 2005;175:5390–5395.
47. Kang HR, Cho SJ, Lee CG, Homer RJ, Elias JA. Transforming growth factor (TGF)-β_1 stimulates pulmonary fibrosis and inflammation via a Bax-dependent, Bid-activated pathway that involves matrix metalloproteinase-12. *J Biol Chem* 2007;282:7723–7732.
48. Park WY, Miranda B, Lebeche D, Hashimoto G, Cardoso WV. FGF-10 is a chemotactic factor for distal epithelial buds during lung development. *Dev Biol* 1998;201:125–134.
49. Bhushan A, Itoh N, Kato S, Thiery JP, Czernichow P, Bellusci S, Scharfmann R. *Fgf10* is essential for maintaining the proliferative capacity of epithelial progenitor cells during early pancreatic organogenesis. *Development* 2001;128:5109–5117.
50. Hart A, Papadopoulou S, Edlund H. *Fgf10* maintains notch activation, stimulates proliferation, and blocks differentiation of pancreatic epithelial cells. *Dev Dyn* 2003;228:185–193.